Effect of band offset on carrier transport and infrared detection in InP quantum dots/Si nano-heterojunction grown by metalorganic chemical vapor deposition technique

Citation	Halder, N. N., Biswas, P., Nagabhushan, B., Kundu, S., Biswas, D., & Banerji, P. (2014). Effect of band offset on carrier transport and infrared detection in InP quantum dots/Si nano-heterojunction grown by metalorganic chemical vapor deposition technique. Journal of Applied Physics, 115(20), 203719. doi:10.1063/1.4880738
DOI	10.1063/1.4880738
Publisher	American Institute of Physics Publishing
Version	Version of Record
Terms of Use	http://cdss.library.oregonstate.edu/sa-termsofuse

Effect of band offset on carrier transport and infrared detection in InP quantum dots/Si nano-heterojunction grown by metalorganic chemical vapor deposition technique

Nripendra N. Halder,[1] Pranab Biswas,[2] B. Nagabhushan,[2] Souvik Kundu,[3] D. Biswas,[4] and P. Banerji[2,a)]

[1]*Advanced Technology Development Centre, Indian Institute of Technology, Kharagpur 721 302, India*
[2]*Materials Science Centre, Indian Institute of Technology, Kharagpur 721 302, India*
[3]*School of Electrical Engineering and Computer Science, Oregon State University, 1148 Kelley Engineering Center, Corvallis, Oregon 97331-5501, USA*
[4]*Department of Electronics & Electrical Communication Engineering, Indian Institute of Technology, Kharagpur 721 302, India*

(Received 23 January 2014; accepted 16 May 2014; published online 30 May 2014)

Epitaxy of III-V semiconductors on Si gets recent interest for next generation system on heterogeneous chip on wafer. The understanding of band offset is thus necessary for describing the charge transport phenomenon in these heterojunctions. In this work, x-ray photoemission spectroscopy has been used to determine the band offsets in a heterojunction made of InP quantum dots on Si. The valence and conduction band offset was found to be 0.12 eV and 0.35 eV, respectively, with a type-II band lineup. Deviation from theoretical prediction and previously published reports on quasi similar systems have been found and analyzed on the basis of the effect of strain, surface energy, shift in the electrostatic dipole and charge transfer at the interface. The carrier transport mechanisms along with different device parameters in the heterojunction have been studied for a temperature range of 180–300 K. This heterojunction is found to behave as an efficient infrared photodetector with an ON/OFF ratio of 21 at a reverse bias of 2 V. The corresponding rise and decay time was found to be 132 ms and 147 ms, respectively. © *2014 AIP Publishing LLC*. [http://dx.doi.org/10.1063/1.4880738]

I. INTRODUCTION

InP is a potential material for various optoelectronic applications due to its direct band gap. It can be used for the generation and detection of terahertz (THz) frequency along with emission in the near infrared (IR) region.[1] By virtue of quantum size effect, the band gap energy of InP can be engineered by the formation of the quantum dots (QDs). As InP is very brittle as well as expensive, it is difficult to handle it in various steps of the device processing. On the other hand, cheap, robust and large diameter wafer is available for Si and it has fully developed microelectronic process technology though being an indirect band gap material it cannot be used for the fabrication of optical sources. Thus, the integration of InP on Si can be a suitable match for the next generation System on Heterogeneous Chip on Wafer (SOHCOW).[2] As InP has large lattice and thermal expansion coefficient mismatch with Si, dislocations and cracks are formed at the grown thin film. However, formation of nanostructures, such as QDs, can minimize the problems related to the dislocations. Tuning the dimensions of the QDs, substantial portion of the electromagnetic spectrum from infrared to visible region can be made to absorb on InP which will eventually enhance the efficiency of a detector made of it. It has been found in the literature that the electrical transport properties are affected by the band offsets of the corresponding semiconductors. While crossing the interfaces, the band offset between the semiconductors acts as a barrier for the charge carriers and it has detrimental effect on the efficiencies of optoelectronic devices such as the conversion efficiency of a heterojunction photovoltaic devices. For example, a solar cell having n-type window with a p-type absorber layer, conduction band offset (ΔE_c) should have a small positive value. For a negative ΔE_c, the built in potential limits the open circuit voltage as well as the conversion efficiency. On the other hand, higher values of ΔE_c can block the electron flow to the window layer.[3] Thus, to analyze the performance of a heterojunction based optoelectronic device, the study of energy band diagram is essential.

X-Ray Photoelectron Spectroscopy (XPS) is a well-known experimental technique for the determination of the band offset in semiconductor heterostructures. It has been seen in the literature that there exists two methods for calculating the band offset from XPS spectra. In the direct technique, continuous measurement of valence band photo electron spectra are taken for the increasing layer thickness. At the interfacial region of the semiconductors, both the valence band leading edges are measured and the valence band offset (ΔE_v) can be calculated from the extrapolation of the corresponding edges. Though the direct method is simple, it cannot be used for all types of interfaces as it requires continuous measurement. On the other hand, the semi-direct technique can be applied for any kind of interfaces. In this technique, the core level XPS spectra are measured at the interface along with the valence band position in all the

a)Author to whom correspondence should be addressed. Electronic mail: pallab@matsc.iitkgp.ernet.in

constituent materials. In the literature, it is found that the semi-direct method has been used to study the band offsets in different heterojunctions like CdTe/CdS,[4] GaAs/AlAs,[5] AlN/Si,[6] and several others.

In this work, we devote ourselves to study the band offsets between InP QD/Si nano-heterojunction by XPS. We shall see later that formation of type-II band lineup has been occurred with very low amount of valance band offset in this system. Due to spatial distribution of electrons and holes in different regions in type-II heterojunction, this type of band lineup is important to form new band gap in the interface and can be used either as a recombination centre or for charge separation.[7] On the other hand the relaxation dynamics indicate that type-II semiconductor heterostructures are ideal for photovoltaic, photoconductive and detector applications due to their ability for long-range photo induced charge separation.[8] Thus, the combined advantage of monolithic integration together with type-II structure can be obtained from InP QD/Si nano-heterostructures. It has been found that the barrier for electrons in the conduction band is much higher than that of holes in the valance band which illustrates that injection of holes from Si to InP is easier than electron injection from InP to Si. The carrier transport as well as the different device parameters has been studied by current voltage measurements at different temperatures. As an example, in the present investigation, we have studied the IR detection property of InP QD/Si nano-heterojunction. In the literature it is found that several Si based nano-heterojunctions with GaN,[9–12] ZnO,[13,14] and InN[15] have been reported for the detection of ultraviolet, visible and infrared photons. So far as the IR detection is concerned, Kumar *et al.*[15] has reported a device based on InN nano-wires/n-Si nano-heterojunction which can detect wavelength higher than 1500 nm. Though Prunchel *et al.*[1] reported a nano-heterojunction made of InP and Si, however, the authors have not investigated the suitability of their device for IR detection rather they reported rectifying current voltage behavior in the heterostructures. Thus, it is found from the literature that IR detectors based on nano-heterojunctions are not well studied. So, in the present work, the IR detection characteristics of the nano-heterojunction is explored to show efficient detection along with low response time which, indeed, is obtained as a result of higher photo-induced charge separation in this type-II nano-heterojunction.

II. EXPERIMENTAL PROCEDURE

InP QDs and thin films have been grown on Si (100) substrates by means of a horizontal atmospheric pressure metalorganic chemical vapor deposition (MOCVD) system. Two sets of samples were grown by changing the growth time. First set of samples were grown for 15 s at a temperature of 560 °C to facilitate formation of the QDs and the other set were grown for 30 min at 600 °C to obtain InP films. Trimethylindium (TMIn) and phosphine (PH_3) were used as the precursors for indium and phosphorus, respectively; and high purity hydrogen was used as the carrier gas. Prior to the growth all the substrates were cleaned using suitable organic solutions for degreasing. Then they were dipped in a chemical solution of 10% HF to etch the native SiO_2. Finally the substrates were rinsed for 5 min in de-ionised water (18.2 MΩ) and dried with nitrogen gun. XPS measurements of the InP thin film, InP QDs/Si and Si were performed by exciting them with X-rays corresponding to Al K_α line (1486.6 eV). The base pressure of the analysis chamber was kept at 10^{-9} torr. The binding energies were corrected with reference to the C 1 s line around 284.50 eV. For the electrical measurements, the ohmic contacts on Si and InP QDs were created by Al and In, respectively. The voltage was measured on applying a current from a constant current source in the temperature range 180–300 K. To study the infrared photo detection property the current voltage characteristics has been measured by illuminating the sample with an infrared lamp (Philips R95-E 100 W/230 V) having wavelength spectrum in the range of 780–1400 nm (IR-A region) with a pronounced peak at approximately 1000 nm and the shorter wavelengths ($\lambda < 900$ nm) were blocked by a high pass filter. The photocurrent measurements of the sample have been performed by illuminating it with infrared radiation in the wavelength region 900–1400 nm. A UV-Vis-NIR spectrophotometer (PerkinElmer LAMBDA 750) was used for this purpose whereas the corresponding current voltage characteristics was measured by a Keithley 4200 semiconductor characterization system.

III. RESULTS AND DISCUSSION

Figure 1 shows the typical surface morphology of the samples grown at 560 °C for 15 s as observed by atomic force microscope (AFM). Distinct QDs having a height and diameter distributions around 3.3 nm and 13 nm, respectively, have been observed. The dot density was found to be around $6.2 \times 10^{14}\,m^{-2}$. The presence of isolated island like dots, as observed from the plan view of the transmission electron microscopic image (inset of Fig. 1), is the signature of the Volmer-Weber type of growth.

Figures 2(a)–2(d) show the core level XPS spectra for In $3d_{5/2}$ and Si 2p, fitted with Shirley background and mixed

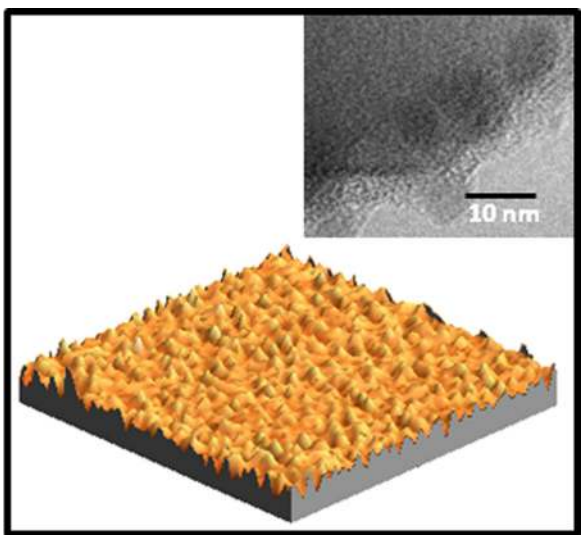

FIG. 1. (a) (1 μm × 1 μm) AFM micrograph showing the surface morphology of the InP QDs grown at 560 °C. The isolated islands in the TEM image (inset) suggest the Volmer-Weber type type of growth.

Lorentzian-Gaussian Voigt function. The In $3d_{5/2}$ spectrum of InP thin film and that of InP/Si nano-heterojunction is assigned to bonding configuration of In-P and is shown in Figs. 2(a) and 2(c), respectively. The Si 2p spectra for Si and InP/Si nano-heterojunction have been shown in Figs. 2(b) and 2(d), respectively. In Figs. 2(e) and 2(f), the valence band spectrum of InP and that of Si has been shown. The valence band maxima with respect to surface Fermi level was obtained from the point where the background and the linear fit of the leading edge of photoemission spectra intersects.

The offset in the valence band in InP QD/Si nano-heterojunction was obtained from the energy separation between the core levels of the materials and the valance band maxima to core level separations. The numerical expressions for valence band offset can be written as

$$E_{VBO}^{InP/Si} = \left(E_{In,3d_{5/2}}^{InP} - E_V^{InP}\right) - \left(E_{Si,2p}^{Si} - E_V^{Si}\right) - \Delta E_{CL}^{InP/Si},$$

where $\Delta E_{CL}^{InP/Si} (= E_{In,3d_{\frac{5}{2}}}^{InP/Si} - E_{Si,2p}^{InP/Si})$ is the difference between the core level spectra of In $3d_{5/2}$ and Si 2p. Here, E_X^Y is the energy of feature X in material Y.[3,6,16] A wide range spectrum showing the core levels of different elements of InP QDs/p-Si heterostructure has been shown in Fig. 3(a). The band offset in the nano-heterostructure obtained from the detailed calculation has been shown in Fig. 3(b). The band offsets are found to be of type-II and the discontinuities are $\Delta E_v = 0.12\,eV$ and $\Delta E_c = 0.35\,eV$. The position of the corresponding Fermi levels from the band edges was estimated from the valance band leading spectra for n-InP and p-Si and has been shown in Fig. 3(c). The band alignment in equilibrium, and with the application of a forward bias are shown in Fig. 3(d). The values of the experimentally obtained band offsets in this study are found to differ from earlier reports by dell'Orto[17] *et al.* and Mahowald *et al.*[18] In those studies, the heterojunction system was formed on depositing Si on InP (110) cleaved surfaces. It is a well known fact that the strain due to the lattice mismatch in the semiconductor heterojunction modifies the atomic position as well as the interatomic distance. As the distance between the nearest neighboring atoms of the different planes of InP is different, the strain due to (100), (110), and (111) surfaces will also be different. On the other hand the effect of strain depends on the thickness of the constituent semiconductors. As the authors[17,18] had grown Si on cleaved InP (110) substrates, the strain might not affect the InP layer. The corresponding theoretical values are 0.03 eV and 0.24 eV, respectively,[19] which are found to be significantly different than those obtained experimentally. It should be mentioned here that while estimating the band offset of the nano-heterostructure, theoretically, it was assumed that the QDs were fully strained. On the other hand, the position of the excited state in the valance band was not taken into account. Thus, the amount of band offsets is found to be different than the theoretically estimated value. The core level spectra for In in our samples have been shifted by some amount from the ideal one. The shift can be explained on the basis of the residual strain in the heterostructure arising due to the QDs. The strain related splitting in the light hole, heavy hole and spin orbit valence bands makes the shift in the atomic core level.[20] It may be mentioned here that various physical phenomena such as interface defects due to large lattice mismatch and shift in the electrostatic dipole at the interface along with charge transfer can affect the XPS core level spectra. During growth of InP, a polar semiconductor on non-polar Si (100) substrates, electrostatic potential will be generated at the interface due to formation of dipole through transfer of protons and accumulation of nuclear charge. Fluctuation in the potential along the interface as a result of surface imperfections of the substrate will result in discontinuity of the average potential (known as electrostatic dipole shift) and its slope (known as charge accumulation). For any particular pair of semiconductors, it will depend strongly on the interface geometry as well as on the crystallographic orientation.[21] On the other hand, local electronic structure around the core level charge carrier can be modified due to Coulombic interaction with the electrons in the valance band.[22] All these physical factors will lead to alteration in the resultant XPS spectra. Thus, the value of the valance band offset, obtained in the present study, is found

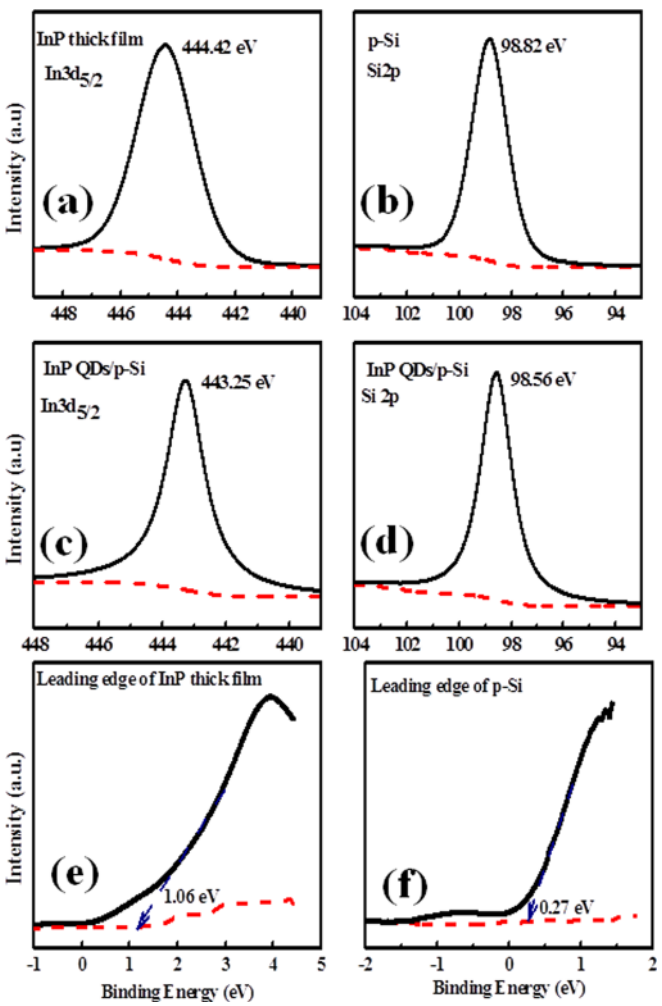

FIG. 2. In $3d_{5/2}$ XPS spectra for (a) InP and (c) InP QDs/Si samples, and Si 2p XPS spectra for (b) Si and (d) InP QDs/Si samples. Experimental data points are fitted by mixed Lorentzian–Gaussian Voigt function with Shirley background. The leading edge of valance band spectra for (e) InP and (f) Si with linear interpolation.

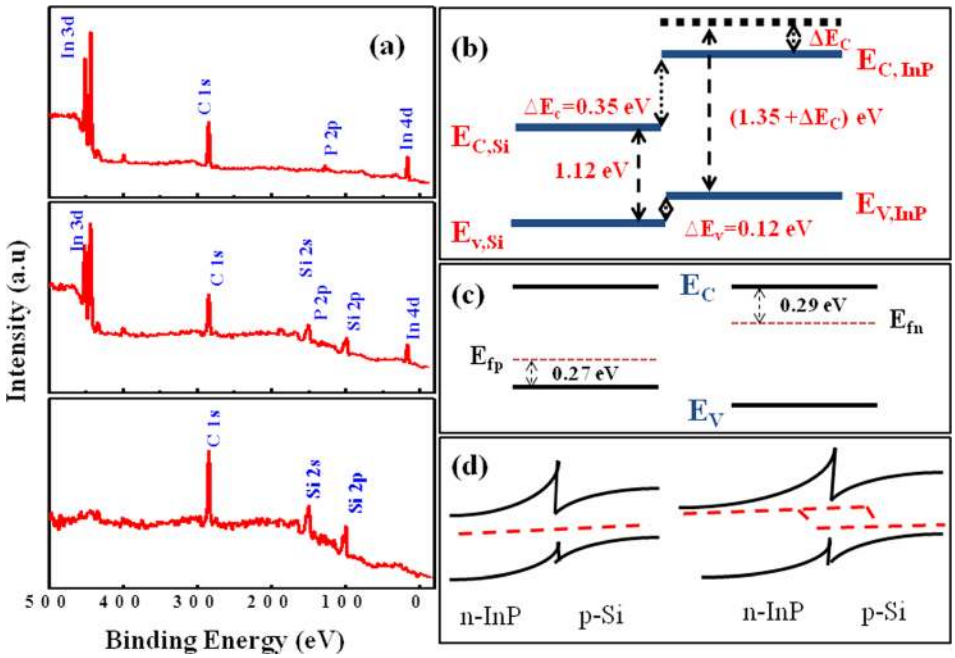

FIG. 3. (a) Wide range XPS spectra of InP QDs/p-Si interface indicating the co-occurrence of different core levels of the constitute semiconductors (b) The valance band maxima and conduction band minima line-up of InP QD/Si nano-heterojunction, showing a type-II band alignment. The dashed lines are the excited states of the carriers occurred due to quantization. (c) Position of Fermi energy levels in p-Si and n-InP from the valance and conduction band edges as measured from the valance band spectra. (d) Band line ups of the heterojunction in equilibrium and under forward bias conditions.

to be different from the earlier works.[17–19] Since InP QD/Si is found to be a type-II heterojunction, the electrons and holes will have their corresponding lowest energy states in InP and Si, respectively. Such property facilitates the charge separation at the heterojunction and thus conducive for various device applications.

Figure 4 shows the current voltage (I-V) characteristics of the InP QDs/Si nano-heterojunction measured at different temperatures. A schematic diagram of the heterojunction has been shown in the lower left inset of Fig. 4. The rectifying characteristic of the curve indicates the formation of a p-n junction. As the back ground doping is unavoidable, InP QDs is as-grown n-type and it creates nano-heterojunction with the host p-Si. The high reverse current ($\sim 10^{-5}$ A) and lower rectification ratio ($\sim$10) at room temperature suggests the thermionic emission dominates in the transport[23] and that the leakage is current due to carrier heating. The rectification ratio was found to be increasing with decrease in temperature while the number of thermally generated carriers decreases. At room temperature, for the low bias condition, the current follows the diode current equation $I = I_0 \exp(\frac{qV}{\eta kT})$, where η is the ideality factor. The current was found to be deviated from linearity at the higher forward bias due to the high series resistance of the p-type Si and high level injection. Since p-Si substrate can be assumed to be a dislocation free single crystal, the recombination via defect states will occur only in the n-InP region. On the other hand, low valance band discontinuity is favorable for injection of holes from p-Si to n-InP rather than the electron injection from n-InP to p-Si.[24,25] Hence, the holes diffuse into the n region overcoming the heterojunction barrier, given by $[qV_D - \Delta E_v - qV]$, where, V_D is the voltage across the diode. The forward current of the heterojunction is a combination of currents occurring from hole diffusion and defect recombination.

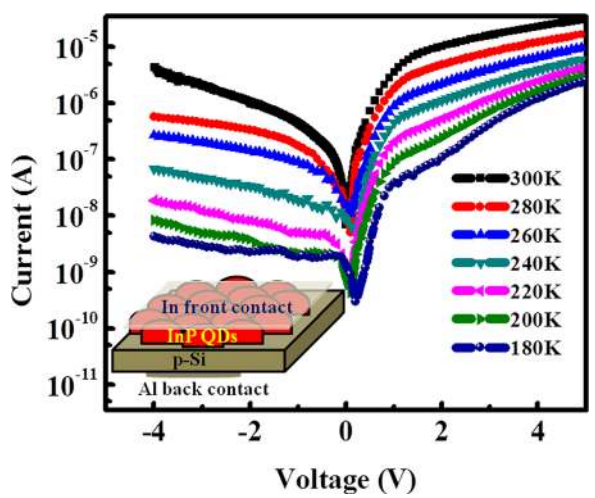

FIG. 4. Current–Voltage characteristics of the n-InP/p-Si in the temperature range 300 K–180 K. (Lower left inset) Schematic diagram of the fabricated heterojunction.

The turn on voltage for the heterojunction in the forward bias has been found to be less than that of a Si homojunction diode presumably coming from the low valence band offset. The turn on voltage was found to be increasing with decrease in temperature. It suggests that the current is dependent on thermionic emission in the low bias condition. In the log (I)–log (V) plot, shown in Fig. 5(a), three distinct regions are observed. At room temperature, in region 1 ($V < 0.3$ V), the current was found to be linearly dependent with the voltage ($I \sim V$) which suggests that the carrier transport is ohmic in nature at (very) low forward bias. In region 2, ($0.3\,V < V < 1.4\,V$), the current increased exponentially obeying $I \approx \exp(\alpha V)$, where α is a constant related to the figure of merit of the diode. In region 3, ($1.4\,V < V < 5\,V$), the current was found to be limited by space charge (SCLC) and follows the relation $I \sim V^{\gamma}$. The dependence of γ, preferably known as SCLC power factor, with temperature has been shown in Fig. 5(b). As the temperature increases from 180 K to 300 K, it is observed that the onset voltage for ohmic to thermionic conduction has reduced from 1 V to 0.3 V. Similarly from

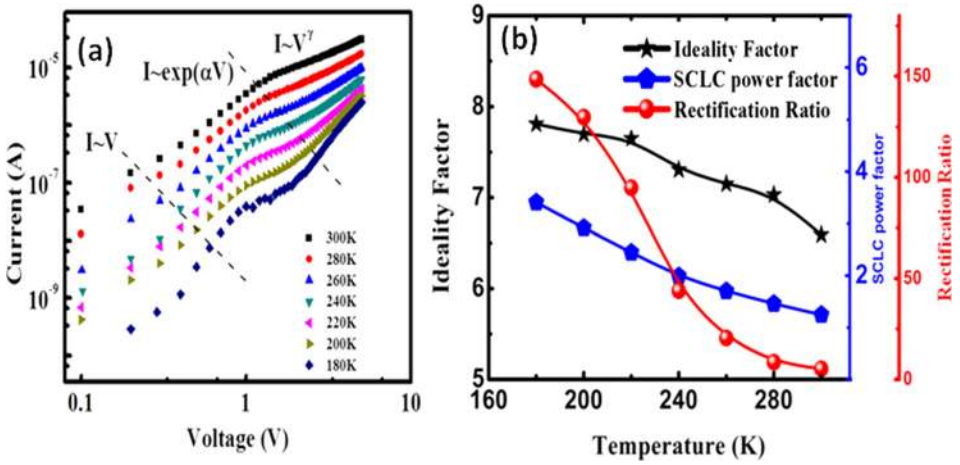

FIG. 5. (a) Log-log plot of the current–voltage under forward bias of n-InP QD/p-Si heterojunction measured at the temperature range 300 K–180 K. The onset of different transport regimes are shown by the dashed lines. (b) Variation of ideality factor, SCLC power factor and rectification ratio with temperature.

thermionic emission to SCLC it is 2.76 V (at 180 K) and gradually decreased to 1.4 V (at 300 K). It is found that the ideality factor changes from 6.6 to 7.8 as the temperature decreases from 300 K to 180 K suggesting deviation from the ideal behavior of the heterojunction. The presence of defect states at the surface as well as at the interface due to large lattice mismatch between InP and Si enhances the recombination. The high ideality factor can be explained through the enhanced recombination current by the coupled defects and donor acceptor recombination.[26]

The space charge limited current governs the transport mechanism for higher forward bias voltage and thus, the current exhibits a weaker dependence on the applied bias voltage (region 3 in Fig. 5(a)). The early saturation of the current of this kind, due to the injection of single carrier (holes here), is possible for such an alignment of the bands discussed earlier. As the barrier for holes in this particular heterojunction is much lesser than that of electrons, the hole dependent current governs the transport in this region. The SCLC power factor γ is found to have increased from 1.25 to 3.4 as the temperature decreases from 300 K to 180 K. The freezing of the thermionic generated carriers with the decrease in temperature gives rise to the enhanced SCLC power factor and enhances the voltage range for the individual region as well. The temperature dependence of the rectification ratio at a constant voltage (± 3 V) has been shown in Fig. 5(b). It is found to increase with decrease in temperature as the reverse current decreases rapidly while the decrease in the forward current in very less. The decrease in the number of thermally generated carriers with temperature decreases the reverse tunneling current. The low value of dark current ($\sim 2\,\mu$A at 2 V reverse bias) even at room temperature can enable the diode to be used as an infrared photodetector.

To study the infrared detection property using this type-II structure, the current voltage measurements have been performed keeping the device both at dark and infrared illuminated conditions. The corresponding current voltage (I-V) characteristics have been shown in Fig. 6(a). A notable change in the reverse current has been observed due to photo generated carriers. For a p-n junction at reverse bias, the photo generated electrons and holes in the depletion region got separated due to the presence of the electric field, giving rise to the current due to minority carriers. The band discontinuities act as barriers for them at the interface. In this present study, as the valance band discontinuity is found to be less than the conduction band discontinuity, the holes from InP will experience a lower barrier than that of electrons from Si while crossing the junction. In essence, the higher conduction band discontinuity will act as an electron blocking layer whereas the holes can move through the junction as the barrier is less. Thus, the transport is due to diffusion of holes from InP QDs to Si. The increase in forward current can be explained by the generation of thermally activated carrier with the infrared illumination.

The response characteristics of the device have been measured by switching the IR illumination source which turned the device ON and OFF. From the transient measurements at three different reverse bias voltages, viz., 1 V, 2 V, and 3 V the ON/OFF ratio were found to be 16, 21, and 23, respectively, and has been shown in Fig. 6(b). The response of the device can be evaluated from the transient photocurrent response characteristics. The rise and decay time (τ_r and τ_d) of the photocurrent response can be estimated from the linear fittings of the transient current in a logarithmic scale (Fig. 6(c)) following $I = I_0(1 - e^{-\frac{t}{\tau_r}})$ and $= I_0 e^{-\frac{t}{\tau_d}}$.[27] The rise and decay are found to be around 132 ms and 147 ms, respectively, at a reverse bias voltage of 2 V. The rapid rise as well as decay suggests that efficient detection can be obtained from type-II band aligned InP QD/Si nano-heterostructure. The ON/OFF ratio is found to be much higher than that of an n-InN/n-Si heterojunction reported by Kumar *et al.*[15] which was type-I by nature. In their study, illuminating the device with photons higher than 1500 nm, the authors reported an ON/OFF ratio of 3.5 at a reverse bias voltage of 5 V with a response time of 150 ms. The increase in the ON/OFF ratio can be explained as the cumulative effect of high photocurrent and low dark current. With the increase in the illumination intensity of the infrared source, the photocurrent is found to increase linearly. It suggests that under illumination carrier density along with conduction of carriers in the nano-heterojunction increases due to the modification of the band profile.[28] However, responsivity ($R = \frac{I_{ph}}{P_{ill}}$) of the detector, defined as the ratio of the steady state photocurrent $I_{ph}(= I_{illuminated} - I_{dark})$ to the incident optical power (P_{ill}), is found to decrease from 2.66 mA/W to 2.23 mA/W when the illuminating power density is increased from 45 mW/cm^2 to 140 mW/cm^2.

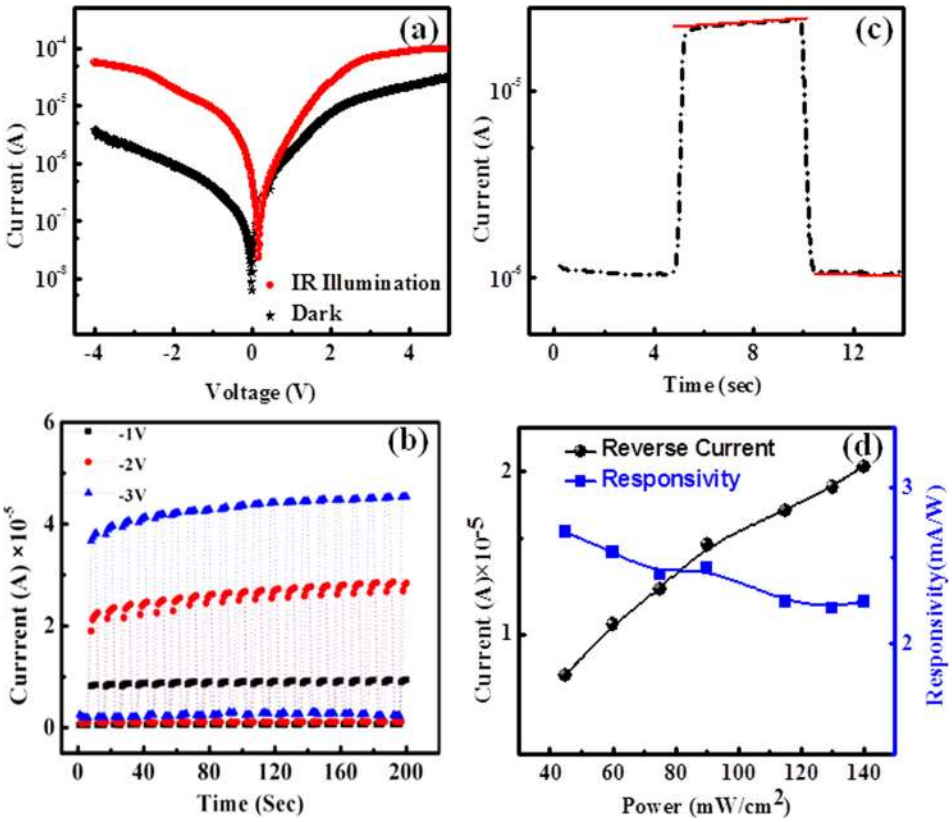

FIG. 6. (a) I-V characteristics of the infrared detector under the dark (black) and infrared (Philips R95-E 100 W/ 230 V lamp) illuminated condition (red). (b) Transient measurement of the ON/OFF current of the device at 1 V (black), 2 V (Red), and 3 V (blue), respectively. (c) A logarithmic plot of transient photocurrent of the device measured at a reverse bias voltage of 2 V. (d) Variation of reverse current and responsivity of the device with illumination power at a reverse bias of 2 V.

The variation of the photocurrent and responsivity with the illumination intensity are shown in Fig. 6(d). The responsivity of the device is comparable to that reported by Elkurdi *et al.*[29] The authors have obtained a value of 3 mA/W for 1.5 μm photon in a device consisting of 20 cycles of Ge QDs embedded in Si. The value of the responsivity could be improved further using multilayered QDs with proper capping.

The variation of the photo generated current with the incident wavelength in the device at a reverse bias voltage of −2 V has been shown in Fig. 7. The photocurrent is found to increase in the wavelength region 1020–1180 nm due to cumulative effect of absorption at Si band edge as well as at the Si/InP QDs interface. As the nano-heterojunction has type-II band line up, new band gap energies can be obtained along with higher spatial separation of photo induced carriers at the interface. The individual effect of absorption of infrared photons and generation of photo induced carriers at Si/InP QDs interface and Si band edge have been shown by two separate regions, viz. R1 and R2, respectively, in Fig. 7. Reduction of the dark current by blocking of electrons by means of conduction band discontinuity gives rise to higher response.

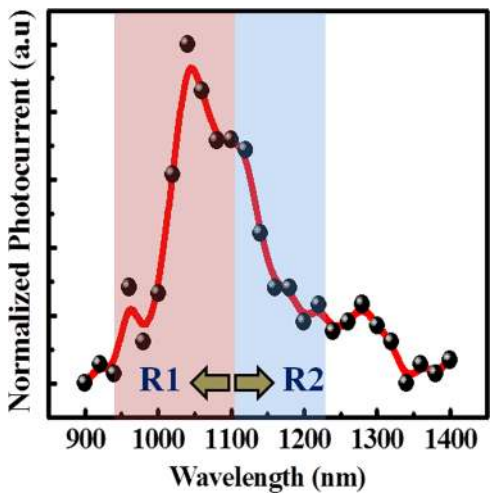

FIG. 7. Normalized photocurrent spectrum of InP QD/Si nano-heterojunction at a reverse bias voltage of −2 V. The individual signature of formation of new band gap at the InP QD/Si interface (R1) and Si band edge (R2) are shown.

IV. CONCLUSION

Thus, in this work, the band offset in a heterojunction made of InP QDs on Si has been determined from the core level XPS spectra. The corresponding heterojunction was found to be type-II. The valence band and conduction band offset was measured to be 0.12 eV and 0.35 eV, respectively. This type of band offset suggests injection of holes from p-Si to n-InP is favorable rather than the reverse one. The structure is found to be an efficient detector for infrared radiation with high ON/OFF ratio and fast response. Compared to type-I structure, type-II heterojunctions have greater efficiency in photo induced carrier separation together with formation of new band gap at the interface. Thus, heterojunction of InP QD on Si is a potential candidate for heteroepitaxial optoelectronic devices.

ACKNOWLEDGMENTS

N. N. Halder thankfully acknowledges financial help from DST, India (Sanction No. 100/IFD/196/2010-11, dated:

03/06/10). The authors are thankful to Mr. P. Chakraborty for his technical help in the growth, Mr. P. Das for his suggestions in transport study and Dr. R. Mukherjee and his group (Department of Chemical Engineering, IIT Kharagpur) for AFM measurements and Dr. T. Shripathi (UGC-DAE CSR, Indore) for XPS measurements.

[1]S. Prucnal, S. Zhou, X. Ou, H. Reuther, M. O. Liedke, A. Mücklich, M. Helm, J. Zuk, M. Turek, K. Pyszniak, and W. Skorupa, Nanotechnology **23**, 485204 (2012).
[2]N. N. Halder, S. Kundu, R. Mukherjee, D. Biswas, and P. Banerji, J. Nanopart. Res **14**, 1279 (2012).
[3]A. M. A. Haleem and M. Ichimura, J. Appl. Phys. **107**, 034507 (2010).
[4]J. Fritsche, A. Thiben, A. Klein, and W. Jaegermann, Thin Solid Films **387**, 158 (2001).
[5]J. R. Waldrop, S. P. Kowalczyk, R. W. Grant, E. A. Kraut, and D. L. Miller, J. Vac. Sci. Technol. B **19**, 573 (1981).
[6]H. Ishikawa, B. Zhang, T. Egawa, and T. Jimbo, Jpn. J. Appl. Phys., Part 1 **42**, 6413 (2003).
[7]P. Peng, D. J. Milliron, S. M. Hughes, J. C. Johnson, A. P. Alivisatos, and R. J. Saykally, Nano Lett. **5**, 1809 (2005).
[8]L. P. Balet, S. A. Ivanov, A. Piryatinski, M. Achermann, and V. I. Klimov, Nano Lett. **4**, 1485 (2004).
[9]W.-Y. Weng, T.-J. Hsueh, S. Chang, S. Wang, H.-T. Hsueh, and G. Huang, IEEE J. Sel. Top. Quantum Electron. **17**, 996 (2011).
[10]L. Rigutti, M. Tchernycheva, A. De Luna Bugallo, G. Jacopin, F. Julien, L. Zagonel, K. March, O. Stephan, M. Kociak, and R. Songmuang, Nano Lett. **10**, 2939–2943 (2010).
[11]A. de Luna Bugallo, M. Tchernycheva, G. Jacopin, L. Rigutti, F. H. Julien, S.-T. Chou, Y.-T. Lin, P.-H. Tseng, and L.-W. Tu, Nanotechnology **21**, 315201 (2010).
[12]K. M. A. Saron, M. R. Hashim, N. Naderi, and N. K. Allam, J. Appl. Phys. **114**, 134510 (2013).
[13]R. Ghosh and D. Basak, Appl. Phys. Lett. **90**, 243106 (2007).
[14]C.-H. Chen, S.-J. Chang, S.-P. Chang, M.-J. Li, I.-C. Chen, T.-J. Hsueh, and C.-L. Hsu, Chem. Phys. Lett. **476**, 69 (2009).
[15]M. Kumar, T. N. Bhat, M. K. Rajpalke, B. Roul, A. T. Kalghatgi, and S. B. Krupanidhi, Nanoscale Res. Lett. **6**, 609 (2011).
[16]E. A. Kraut, R. W. Grant, J. R. Waldrop, and S. P. Kowalczyk, Phys. Rev. B **28**, 1965 (1983).
[17]T. dell'Orto, G. D. Stasio, M. Capozi, C. Ottaviani, C. Quaresima, P. Perfetti, Y. Hwu, and G. Margaritondo, Phys. Rev. B **48**, 8035 (1993).
[18]P. H. Mahowald, R. S. List, J. Woicik, P. Pianetta, and W. E. Spicer, Phys. Rev. B **34**, 7069 (1986).
[19]N. N. Halder, P. Biswas, T. D. Das, S. K. Das, S. Chottopadhyay, D. Bisas, and P. Banerji, J. Appl. Phys. **115**, 043101 (2014).
[20]E. T. Yu, E. T. Croke, D. H. Chow, D. A. Collins, M. C. Phillips, T. C. McGill, J. O. McCaldin, and R. H. Miles, J. Vac. Sci. Technol. B **8**, 908 (1990).
[21]W. A. Harrison, E. A. Kraut, J. R. Waldrop, and R. W. Gran, Phys. Rev. B **18**, 4404 (1978).
[22]K. Okada, A. Kotani, and B. T. Thole, J. Electron. Spectrosc. Relat. Phenom. **58**, 325 (1992).
[23]F. Chen, B. A. Orner, A. Khan, P. R. Berger, S. Ismat Shah, and J. Kolodzey, IEEE Electron Device Lett. **17**, 589 (1996).
[24]M. Willander, G. D. Shen, D. X. Xu, and W. X. Ni, J. Appl. Phys. **63**, 5036 (1988).
[25]G. Wu, G. Du, F. Gao, H. Wang, C. Shen, and W. Li, J. Phys. D: Appl. Phys. **45**, 215102 (2012)
[26]A. Schenk and U. Krumbein, J. Appl. Phys. **78**, 3185 (1995).
[27]N. V. Joshi, *Photoconductivity: Art, Science, and Technology* (Dekker, New York, 1990).
[28]H. Zhang, A. V. Babichev, G. Jacopin, P. Lavenus, F. H. Julien, A. Yu. Egorov, J. Zhang, T. Pauporté, and M. Tchernycheva, J. Appl. Phys. **114**, 234505 (2013).
[29]M. Elkurdi, P. Boucaud, S. Sauvage, O. Kermarrec, Y. Campidelli, D. Bensahel, G. Saint-Girons, and I. Sagnes, Appl. Phys. Lett. **80**, 509 (2002).